



Vine Copula Data Fusion for Failure Probability Analysis of Steel Bridge Girder Section

Xueping Fan, M.ASCE¹ and Yuefei Liu²

Abstract: For steel bridge girders, several control sections usually exist. If one or more sections fail, then the bridge girder might fail. Therefore, the failure probability analysis of each control section is important for bridge girder safety assessment. To make a reasonable failure probability analysis for bridge girder sections that have structural health monitoring data, first, vine copula models that consider the nonlinear correlation of multiple monitored variables will be established based on the extreme stress data of bridge girder sections, which mean that the extreme stress data fusion will be achieved; second, the vine copula models that consider the nonlinear correlation of failure modes of the multiple monitored points from bridge girder sections that were constructed with the corresponding performance functions, further, by combining the built vine copula models with the first-order second-moment (FOSM) method, the failure probability of the bridge girder section that considers the nonlinear correlation of failure modes at the multiple monitored points will be analyzed; finally, the monitored data of an existing bridge will be provided to illustrate the proposed model and method. The results show that: (1) the C-vine structure-based failure probability of a bridge girder is smaller than the D-vine structure-based failure probability; (2) the obtained bridge girder section failure probability that considered the nonlinear correlation of the failure modes is smaller than when the correlation of the failure modes is not considered. It was illustrated that the obtained C-vine structure-based failure probability was the most reasonable. DOI: [10.1061/\(ASCE\)BE.1943-5592.0001709](https://doi.org/10.1061/(ASCE)BE.1943-5592.0001709). © 2021 American Society of Civil Engineers.

Author keywords: Bridge girder section; Nonlinear correlation; Vine copula model; First-order second-moment method; Reliability analysis.

Introduction

Bridge health monitoring (BHM) systems have produced a large amount of monitored data on long-term service periods. How to reasonably analyze the bridge failure probability using these data is in the initial research stages, but it is one of the main scientific problems and consensus problems in the BHM field (Fan 2014; Frangopol et al. 2008a; Strauss et al. 2016).

Bridge reliability research mainly computes bridge component reliability or bridge system reliability with the reasonable reliability analysis methods [e.g., the first-order second-moment reliability method (FOSM)(Fan 2014; Ang and Tang 2007; Dissanayake and Karunamanda 2008; Melchers 1987; Fan and Liu 2018a; Dai and Cao 2017; Suda et al. 2009; Zimmermann et al. 2012), and first-order reliability method (Ang and Tang 2007; Melchers 1987)] based on the general resistance information (e.g., allowable stress and allowable deflection) and general load effect information (e.g., everyday extreme stress and everyday extreme deflection). In this paper, the bridge girder section is adopted as the research

object. The failure probability at the single monitoring point from the bridge girder section is defined as the component failure probability, and the failure probability at the bridge girder section that does and does not consider the correlation of multiple monitored points is considered as the system failure probability. This paper assumes that the failure mode for any monitoring point of the bridge girder section is that the monitored extreme stress is larger than the allowable stress.

Based on BHM data, some research into bridge reliability (or failure probability) was conducted (Fan 2014; Frangopol et al. 2008a; Dissanayake and Karunamanda 2008; Ni et al. 2006; Frangopol et al. 2008b; Catbas et al. 2008; Strauss et al. 2008). However, most of this research assumed that the failure modes at different monitoring points of the bridge girder were independent of each other, and the solved bridge reliability indices were conservative (Fan 2014). For each bridge girder section, due to the same input variables (e.g., vehicle loads and environmental loads), linear or nonlinear correlation between output variables exist (i.e., extreme stress) at different monitored points, furthermore, correlation occurs between the failure modes at different monitored points (Liu 2015; Liu et al. 2014; Liu and Lu 2014; Liu and Fan 2016a, b). Nonlinear correlations generally contain the properties of linear correlation. Therefore, nonlinear correlation plays an important role in the reliability analysis of bridge girder sections. In bridge reliability (or failure probability), some studies into bridge failure probability that considered nonlinear correlation of failure modes at different monitored points have been conducted with copula functions, for example: Fan and Liu provided a new model named by Bayesian Dynamic Gaussian Copula Model (BDGCM) to characterize the time-variant nonlinear correlation between the failure modes of two monitored points and solved the time-dependent failure probability of a bridge system that considered nonlinear correlation between

¹Associate Professor, Key Laboratory of Mechanics on Disaster and Environment in Western China (Lanzhou Univ.), Ministry of Education of China; School of Civil Engineering and Mechanics, Lanzhou Univ., Lanzhou 730000, P. R. China (corresponding author). Email: fanxp@lzu.edu.cn

²Associate Professor, Key Laboratory of Mechanics on Disaster and Environment in Western China (Lanzhou Univ.), Ministry of Education of China; School of Civil Engineering and Mechanics, Lanzhou Univ., Lanzhou 730000, P. R. China. Email: yfliu@lzu.edu.cn

Note. This manuscript was submitted on September 17, 2020; approved on December 16, 2020; published online on March 24, 2021. Discussion period open until August 24, 2021; separate discussions must be submitted for individual papers. This technical note is part of the *Journal of Bridge Engineering*, © ASCE, ISSN 1084-0702.

two failure modes (Fan and Liu 2018b); Wang and Lin analyzed the time-independent failure probability of a continuous girder bridge by considering the nonlinear correlation between failure modes at two points with a copula function (Wang and Lin 2017); Liu and Fan conducted research into time-independent failure probability of a simply supported cored slab bridge (series-parallel system) with mixed copula functions, in the analysis processes only the nonlinear correlation between failure modes at two adjacent points was taken into account (Liu and Fan 2016a); Liu and Fan proposed the Gaussian copula-Bayesian dynamic linear model-based time-dependent failure probability prediction method for Yitong River Bridge, Changchun, China (a flying swallow profiled concrete-filled steel tube arch bridge) that considered the dynamic nonlinear correlation between failure modes at two monitored points (Liu and Fan 2016b). The previous studies show that the given bridge failure probability analysis methods only considered nonlinear correlation between two failure modes. However, the actual bridge girder section commonly has multiple failure modes such as, each section of a bridge girder has multiple monitored points, each monitored point has a failure mode. How to build a nonlinear correlation model for the multiple failure modes, and further assess bridge girder section failure probability should be studied further.

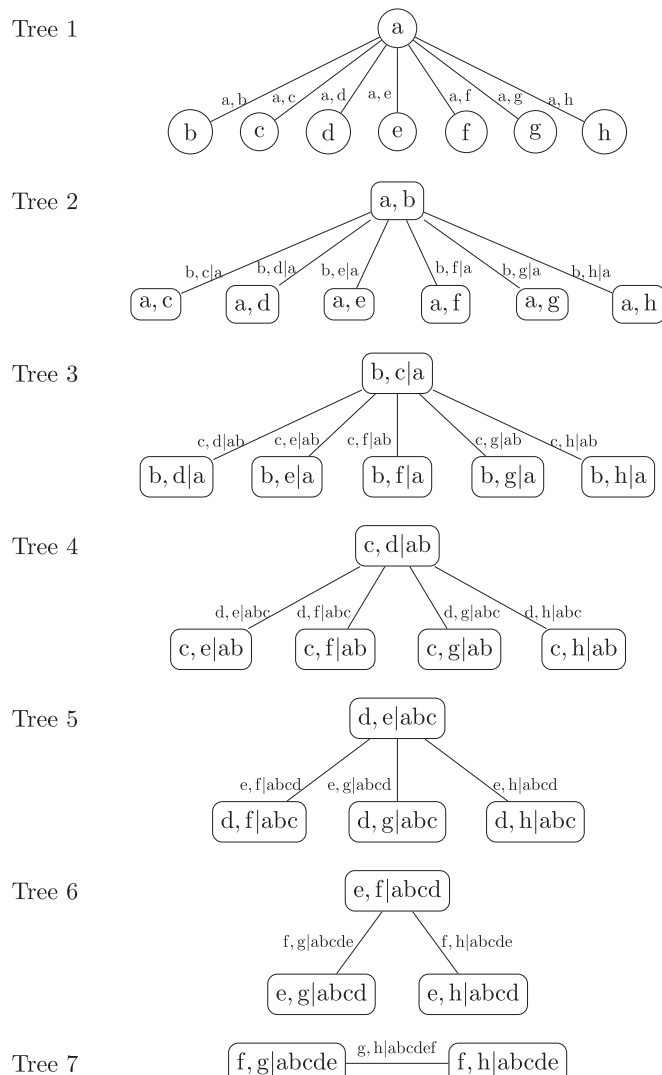


Fig. 1. Eight-dimensional C-vine structure.

Based on the previously discussed existing problems, this paper uses the bridge girder section as the research object, adopts a vine copula model to build the nonlinear correlation model of multiple failure modes at multiple monitored points based on everyday extreme stress data, and further analyzes bridge girder section failure probability. The contents are as follows: (1) based on monitored everyday extreme stress data, the vine copula model of multiple monitored variables (e.g., everyday extreme stress) for a bridge girder section is built (refer the “Vine Copula Model of Multiple Monitored Variables” section); (2) combining the built vine copula model with the FOSM method and the performance functions at multiple monitored points, the failure probability analysis method of a bridge girder section is given (refer the “Failure Probability Analysis of Bridge Girder Section that Considers the Nonlinear Correlation of Failure Modes” section); (3) the monitored data of an actual bridge is provided to illustrate the feasibility and application of the proposed model and method (refer the “Application to an Existing Bridge” section); and (4) some valuable conclusions are summarized (refer the “Conclusions” section). The innovation of this paper was to analyze the bridge girder section failure probability using a vine copula model and extreme stress data for the first time, to the best of the authors’ knowledge, and provides the application method for bridge failure probability analysis.

Vine Copula Model of Multiple Monitored Variables

For the BHM system, each section of a bridge girder has multiple monitored points that correspond to multiple output monitored variables. In this paper, the output monitored variables refer to everyday extreme stresses at the multiple monitored points. Due to the same input random resources including vehicle loads and environmental loads, nonlinear correlation exists between the output random variables. In Section 2, the vine copula model that considered the nonlinear correlation of output

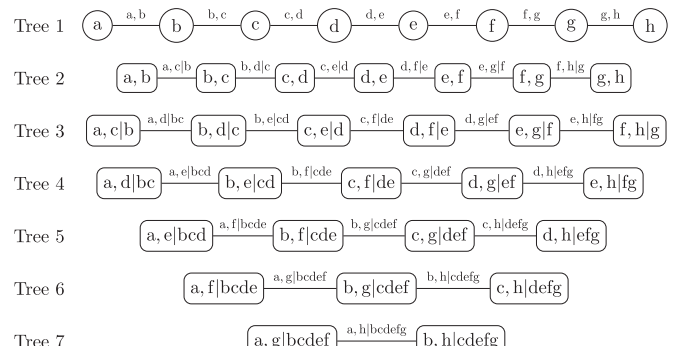


Fig. 2. Eight-dimensional D-vine structure.



Fig. 3. A view of Fumin bridge. (Image by Xueping Fan)

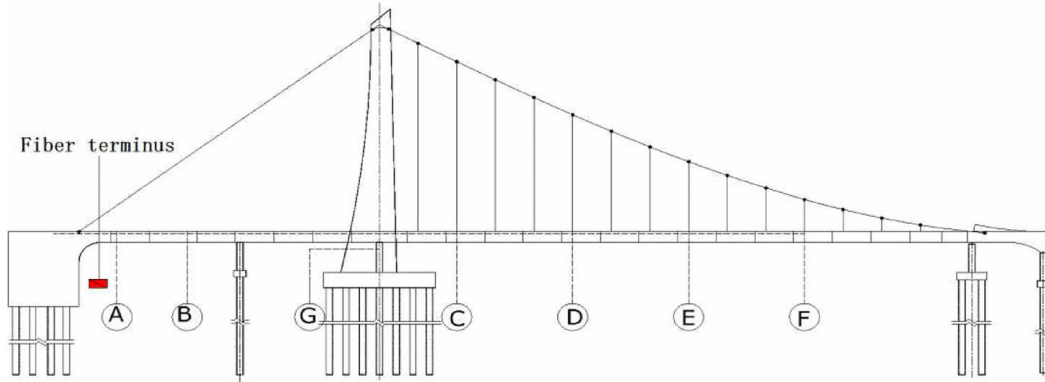


Fig. 4. Seven monitored sections of the steel box girder system.

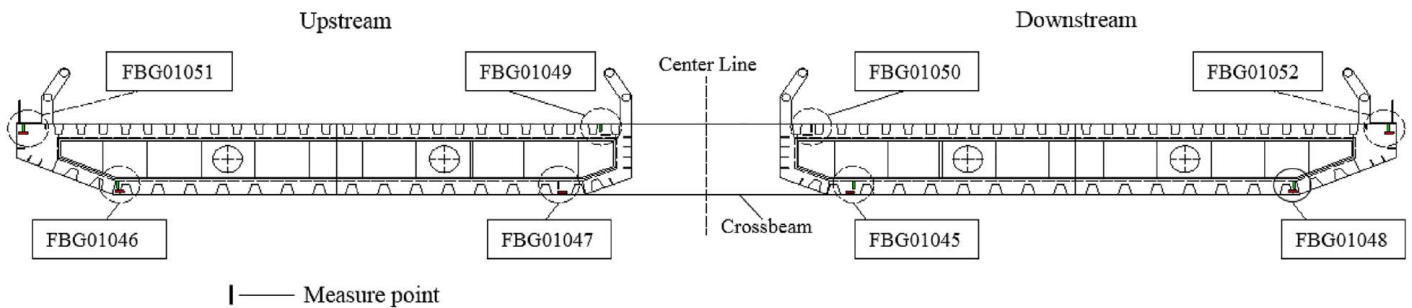


Fig. 5. Monitored sections and the stress sensors of section B.

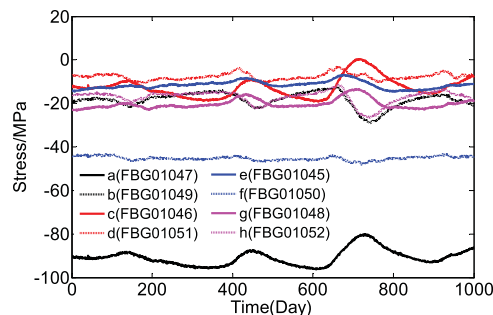


Fig. 6. Data for the eight monitored points.

variables was built based on pair-copula theory and bivariate copula theory.

Pair-Copula Theory

Bedford and Cooke proposed the joint probability distribution function of multivariate random variables based on a pair-copula construction module (Bedford and Cooke 2001, 2002). The pair-copula construction module provides a method to separate the dependence between multidimensional random variables. It considers the nonlinear correlation between two random variables. It decomposes the multidimensional random variables into a number of pair-copula modules. Therefore, it provides a theoretical foundation for the application of vine copula theory in high dimensional random variables.

In this paper, the monitored extreme stresses that corresponded to the n monitoring points from a bridge girder section are defined as the n -dimensional random variable $\bar{X} = (x_1, x_2, \dots, x_n)$, according to the conditional probability density function theory (Ang and Tang 2007), copula model-based joint probability density function $f(x_1, x_2, \dots, x_n)$ can be written as

$$f(x_1, x_2, \dots, x_n) = c(F_1(x_1), F_2(x_2), \dots, F_n(x_n)) \prod_{i=1}^n f_i(x_i) \quad (1)$$

where c = copula density function; and $F_i(x_i)$ and $f_i(x_i)$ = cumulative distribution function (CDF) and probability density function (PDF) of x_i , respectively.

With Eq. (1), the bivariate joint PDF can be obtained

$$f(x_i, x_j) = c_{ij}(F_i(x_i), F_j(x_j))f_i(x_i)f_j(x_j), \quad i, j = 1, 2, \dots, n, \text{ and } i \neq j \quad (2)$$

The following equation, which is conditional PDF, can be obtained:

$$f(x_i|x_j) = c_{ij}(F_i(x_i), F_j(x_j))f_i(x_i), \quad i, j = 1, 2, \dots, n, \text{ and } i \neq j \quad (3)$$

With Eq. (3), the PDF at random variable x conditional on n -dimensional random variables \bar{u} can be obtained with

$$f(x|\bar{u}) = c_{xu_i|\bar{u}_{-i}}(F(x|\bar{u}_{-i}), F(u_i|\bar{u}_{-i}))f(x|\bar{u}_{-i}) \quad (4)$$

where u_i = the i th variable of n -dimensional random variables \bar{u} ; \bar{u}_{-i} = the $n-1$ -dimensional random variables obtained

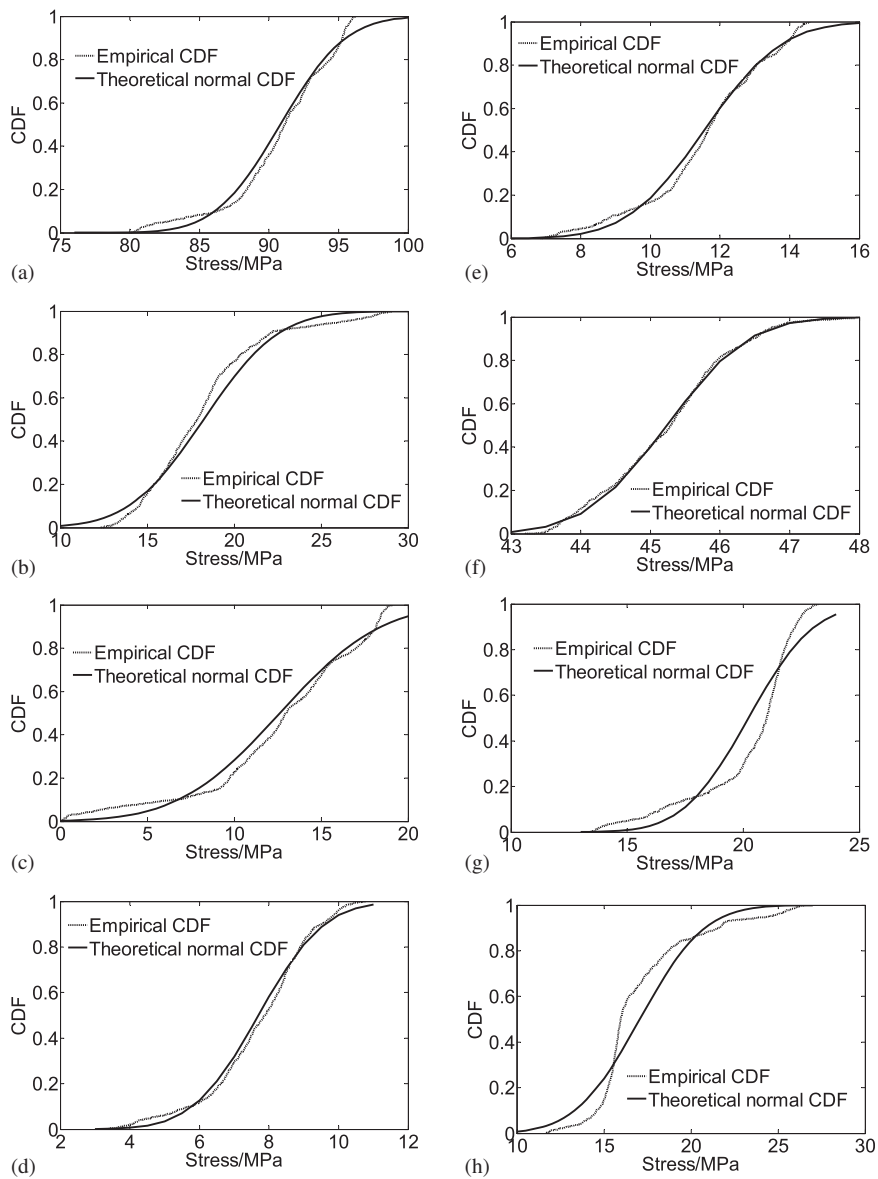


Fig. 7. K-S test results about the monitored stress data of the eight monitored points: (a) K-S test curve of the stress at a (FBG01947); (b) K-S test curve of the stress at b (FBG01949); (c) K-S test curve of the stress at c (FBG01946); (d) K-S test curve of the stress at d (FBG01951); (e) K-S test curve of the stress at e (FBG01945); (f) K-S test curve of the stress at f (FBG01950); (g) K-S test curve of the stress at g (FBG01948); and (h) K-S test curve of the stress at h (FBG01952).

through removing the i th variable from n -dimensional random variables \mathbf{u} .

Bivariate Gaussian Copula Model

In this section, the widely used bivariate Gaussian copula model was adopted to build the nonlinear correlation model between two random variables (Liu 2015; Nelsen 2006). The CDF and PDF about the bivariate Gaussian copula model are respectively shown in

$$\begin{aligned} C(u_1, u_2; \rho) &= \Phi_G(\Phi^{-1}(u_1), \Phi^{-1}(u_2); \rho) \\ &= \int_{-\infty}^{\Phi^{-1}(u_1)} \int_{-\infty}^{\Phi^{-1}(u_2)} \frac{1}{2\pi(1-\rho^2)^{1/2}} \\ &\times \exp\left(-\frac{(r^2 - 2\rho rs + s^2)}{2(1-\rho^2)}\right) dr ds \quad (5) \end{aligned}$$

$$\begin{aligned} c(u_1, u_2; \rho) &= \frac{1}{\sqrt{1-\rho^2}} \\ &\times \exp\left(\frac{\Phi^{-1}(u_1)^2 + \Phi^{-1}(u_2)^2 - 2\rho\Phi^{-1}(u_1)\Phi^{-1}(u_2)}{2(1-\rho^2)}\right) \\ &\times \exp\left(-\frac{\Phi^{-1}(u_1)^2\Phi^{-1}(u_2)^2}{2}\right) \quad (6) \end{aligned}$$

where $u_i = F_i(x_i)$, $i = 1, 2$, $F_i(x_i)$ = the marginal CDF of x_i ; Φ = standard normal CDF; and ρ restricted to the interval $[-1, 1]$ = the relevant parameters of Gaussian copula function.

Pearson's linear correlation coefficient is a measure of the linear correlation between the random variables (Liu 2015). In this paper, Pearson's linear correlation coefficient was used to determine the relevant parameter ρ of bivariate Gaussian copula function. Bivariate Gaussian copula functions include the unconditional bivariate

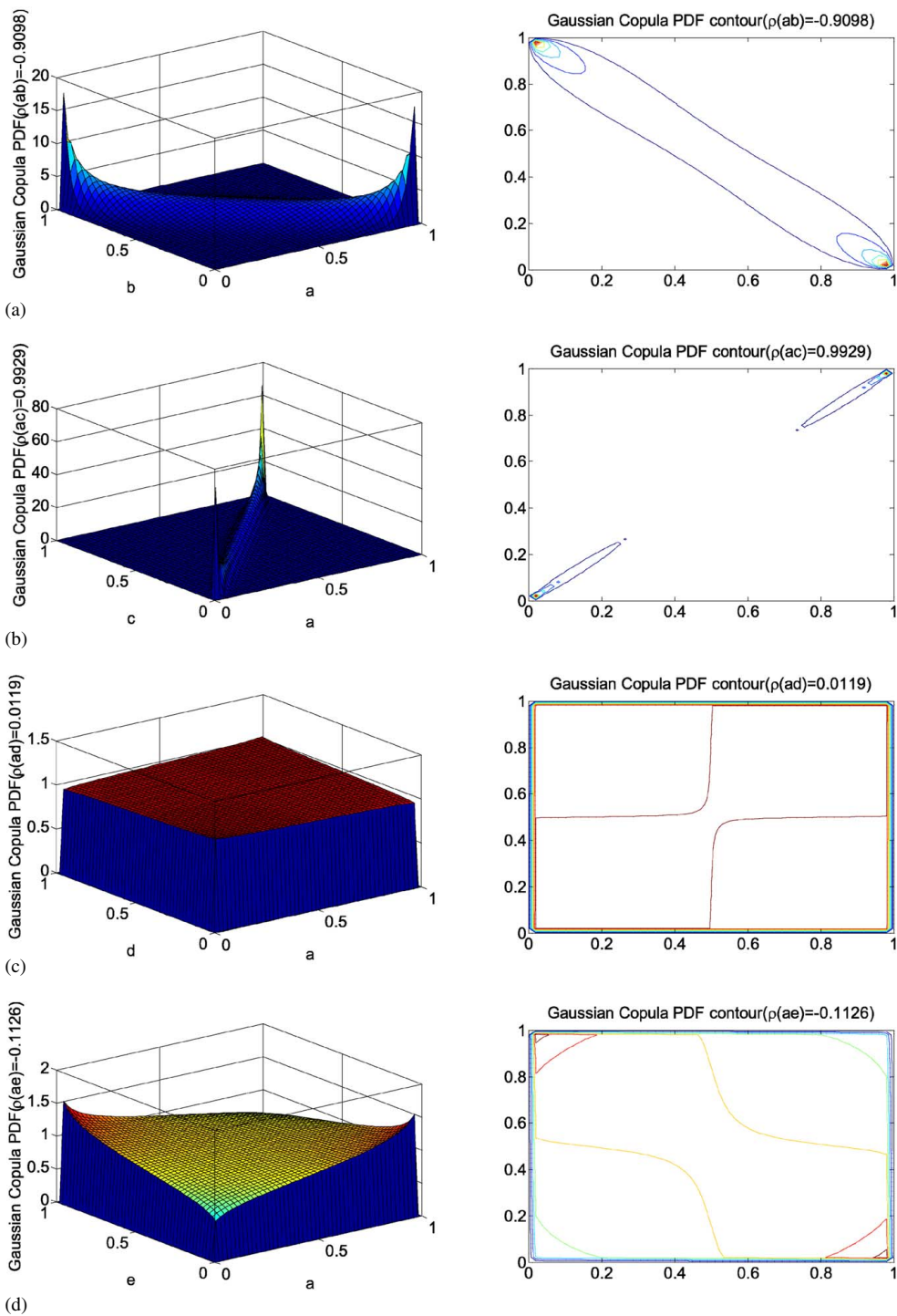


Fig. 8. PDF and contour plots of Gaussian copula functions for C-vine structure: (a) PDF and contour plots of Gaussian copula functions for C_{ab} ; (b) PDF and contour plots of Gaussian copula functions for C_{ac} ; (c) PDF and contour plots of Gaussian copula functions for C_{ad} ; (d) PDF and contour plots of Gaussian copula functions for C_{ae} ; (e) PDF and contour plots of Gaussian copula functions for C_{ag} ; (f) PDF and contour plots of Gaussian copula functions for C_{ah} ; (g) PDF and contour plots of Gaussian copula functions for C_{bca} ; (h) PDF and contour plots of Gaussian copula functions for $C_{be|a}$; (i) PDF and contour plots of Gaussian copula functions for $C_{bf|a}$; (j) PDF and contour plots of Gaussian copula functions for $C_{bg|a}$; (k) PDF and contour plots of Gaussian copula functions for $C_{ch|a}$; (l) PDF and contour plots of Gaussian copula functions for $C_{bh|a}$; (m) PDF and contour plots of Gaussian copula functions for $C_{cd|ab}$; (o) PDF and contour plots of Gaussian copula functions for $C_{ce|ab}$; (p) PDF and contour plots of Gaussian copula functions for $C_{cf|ab}$; (q) PDF and contour plots of Gaussian copula functions for $C_{cg|ab}$; (r) PDF and contour plots of Gaussian copula functions for $C_{ch|ab}$; (s) PDF and contour plots of Gaussian copula functions for $C_{de|abc}$; (t) PDF and contour plots of Gaussian copula functions for $C_{df|abc}$; (u) PDF and contour plots of Gaussian copula functions for $C_{dg|abc}$; (v) PDF and contour plots of Gaussian copula functions for $C_{dh|abc}$; (w) PDF and contour plots of Gaussian copula functions for $C_{ef|abcd}$; (x) PDF and contour plots of Gaussian copula functions for $C_{fg|abcde}$; (y) PDF and contour plots of Gaussian copula functions for $C_{eh|abcde}$; (z) PDF and contour plots of Gaussian copula functions for $C_{fh|abcde}$; and (bb) PDF and contour plots of Gaussian copula functions for $C_{gh|abcdef}$.

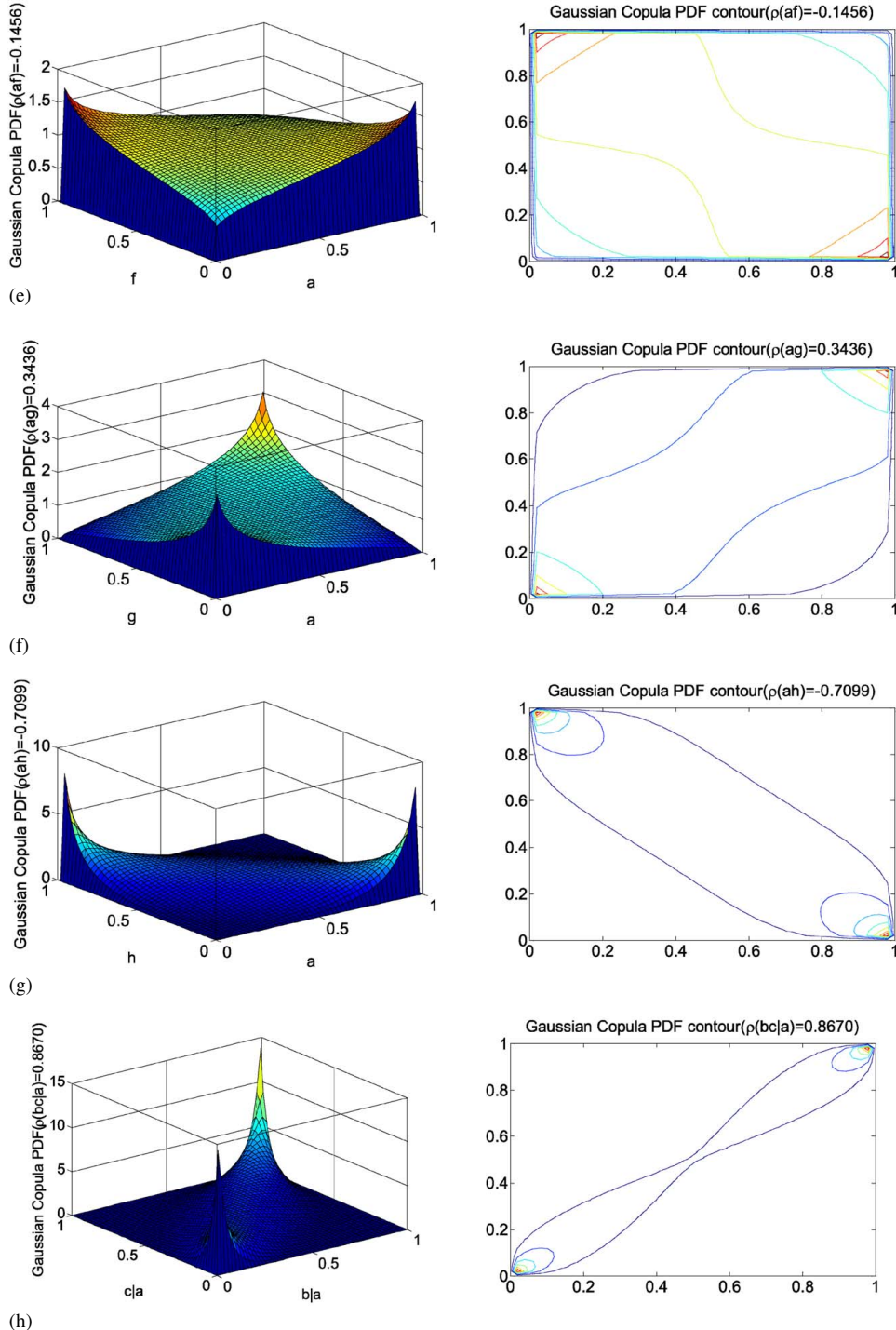


Fig. 8. (Continued.)

Gaussian copula functions and the conditional bivariate Gaussian copula functions.

Assume that Pearson's linear correlation coefficient of any two random variables x_1 and x_2 is expressed with $\rho(1, 2)$. The equation of relevant parameters of the unconditional Gaussian Copula function can be obtained with

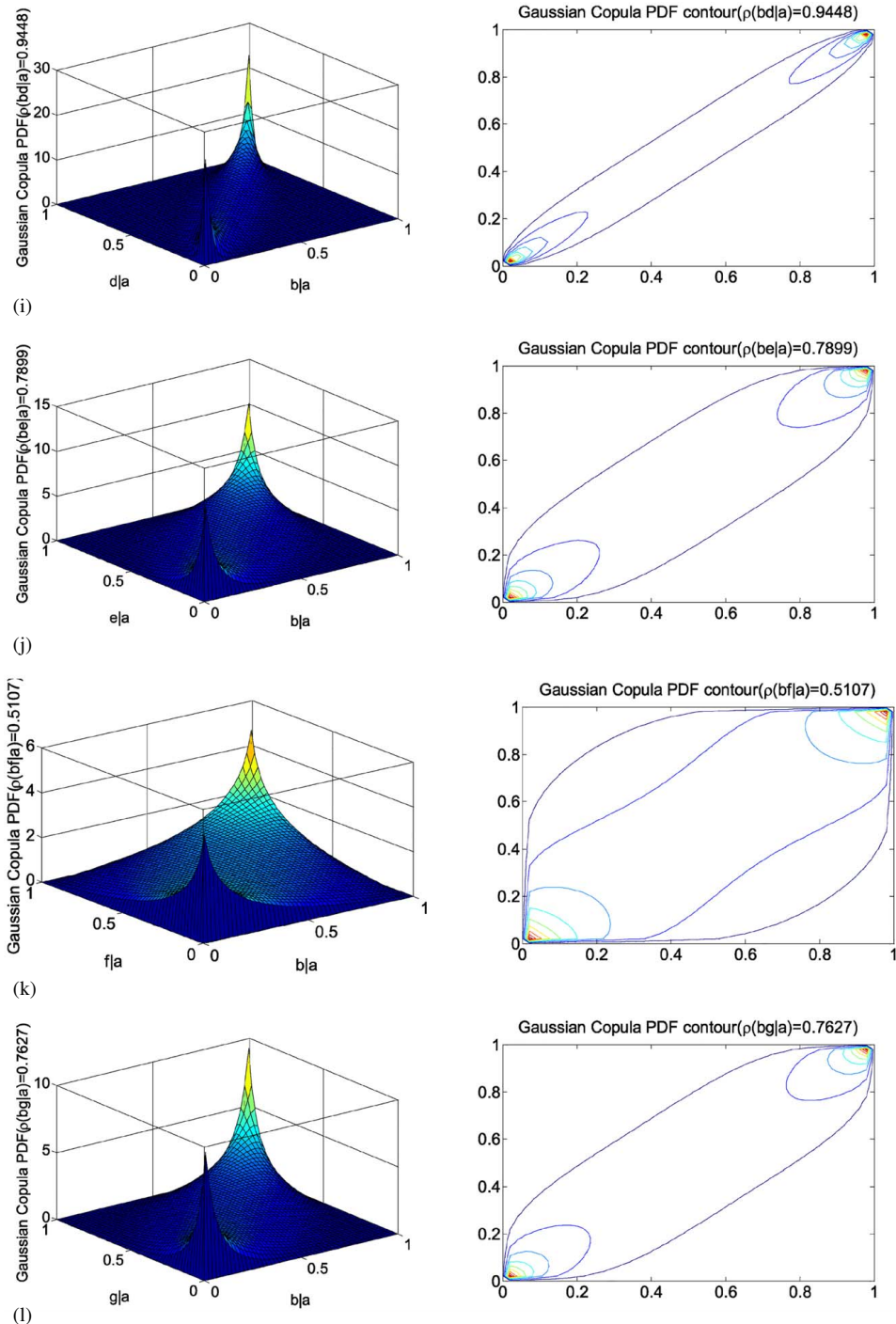
$$\begin{aligned} \rho_{1,2} &= \rho(\Phi^{-1}(u_1), \Phi^{-1}(u_2)) = \rho(\Phi^{-1}(F_1(x_1)), \Phi^{-1}(F_2(x_2))) \\ &= \rho(x_1, x_2) = \rho(1, 2) \end{aligned} \quad (7)$$

The equation of relevant parameters of the conditional Gaussian Copula function can be obtained with

$$\rho_{1,2|3,\dots,n} = \frac{\rho_{1,2|4,\dots,n} - \rho_{1,3|4,\dots,n} \cdot \rho_{2,3|4,\dots,n}}{\sqrt{1 - \rho_{1,3|4,\dots,n}^2} \cdot \sqrt{1 - \rho_{2,3|4,\dots,n}^2}} \quad (8)$$

Vine Copula Model

According to the definition of vine structures (Bedford and Cooke 2001, 2002), each vine is composed of multiple trees, each tree

**Fig. 8. (Continued.)**

contains multiple nodes, each node represents a random variable, the line that connects two nodes is called the edge, different edges (lines) are independent of each other. Different vine structures have different properties. The commonly used one is a regular vine structure that includes many types (Bedford and Cooke 2001, 2002). The commonly used regular vine structure types are C-vine and D-vine. This section uses eight-dimensional random variables (eight-dimensional extreme stresses) as the example to build C-vine structure and D-vine structures, respectively as shown in Figs. 1 and 2. Fig. 1 shows that the C-vine structure of eight-dimensional random variables has seven trees, each tree has one main node. For each tree, the main node is connected to the other nodes. Each line that connects the main node to another node corresponds to one pair-copula model, different lines are

independent of the other. Fig. 2 shows that the D-vine structure of eight-dimensional random variables has 7 trees and 28 edges; each edge corresponds to one pair-copula model.

For the C-vine structure and D-vine structure, the pair-copula models from the first tree are all unconditional pair-copula models, and the pair-copula models from the other trees are all conditional pair-copula models.

Failure Probability Analysis of Bridge Girder Section that Considers the Nonlinear Correlation of Failure Modes

In this section, reliability indices and failure probability about monitored points are solved with the FOSM method (See Sections 3.1

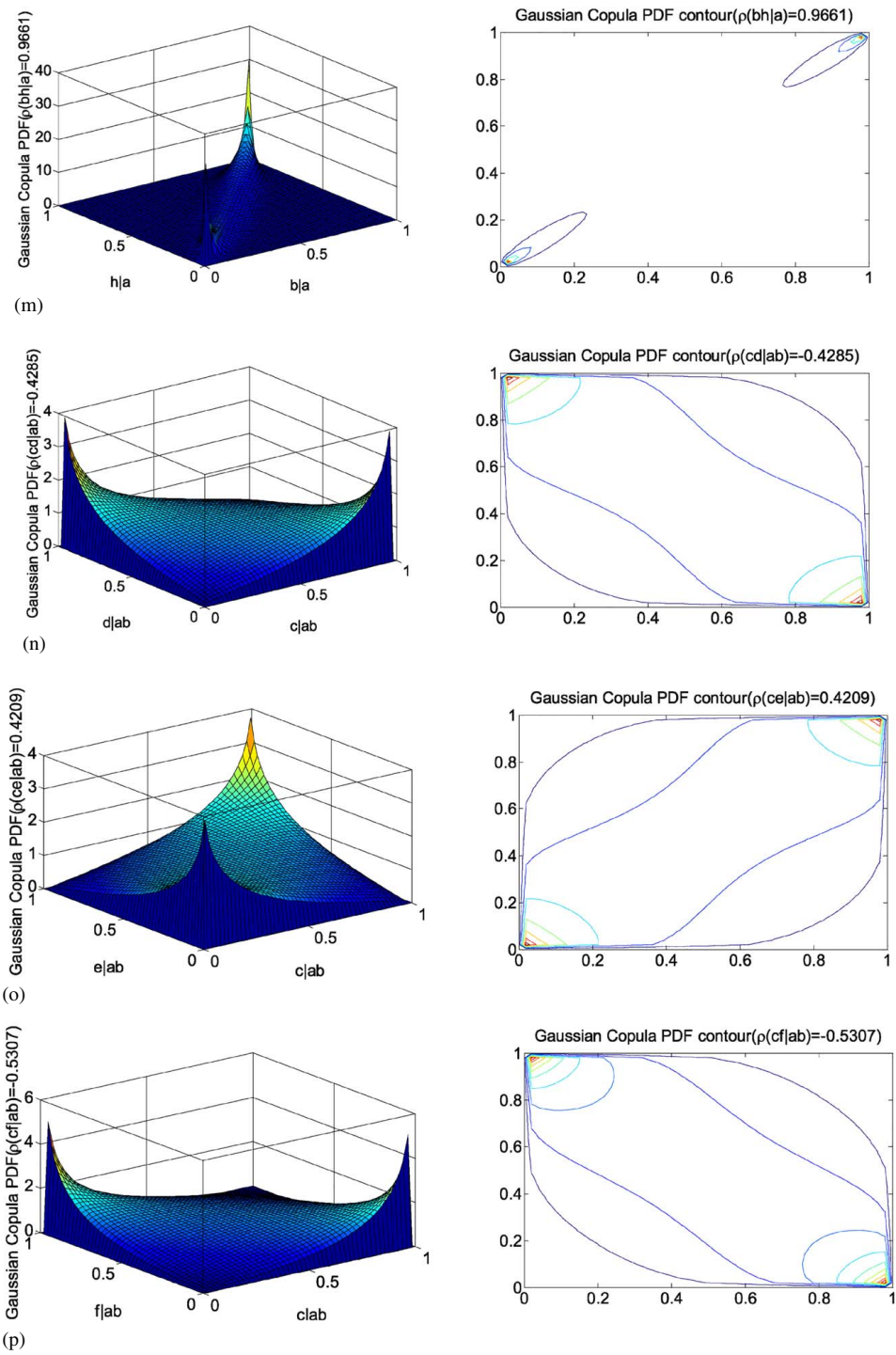


Fig. 8. (Continued.)

and 3.2). Failure probability of bridge section is computed through Section 3.3.

FOSM Method

Assume that there are a strength variable (R) and stress variable (S) that are mutually independent, the mean value and standard variances of which are, respectively μ_R , σ_R and μ_S , σ_S .

For R and S , the theoretical limit state function is

$$g(R, S) = R - S \quad (9)$$

Using the FOSM method (Ang and Tang 2007; Melchers 1987), the computation formula of reliability indices can be obtained with

$$\beta = \frac{\mu_R - \mu_S}{\sqrt{\sigma_R^2 + \sigma_S^2}} \quad (10)$$

Failure Probability Formula of Multiple Monitored Points

In this paper, each monitored point of a bridge girder section has a performance function

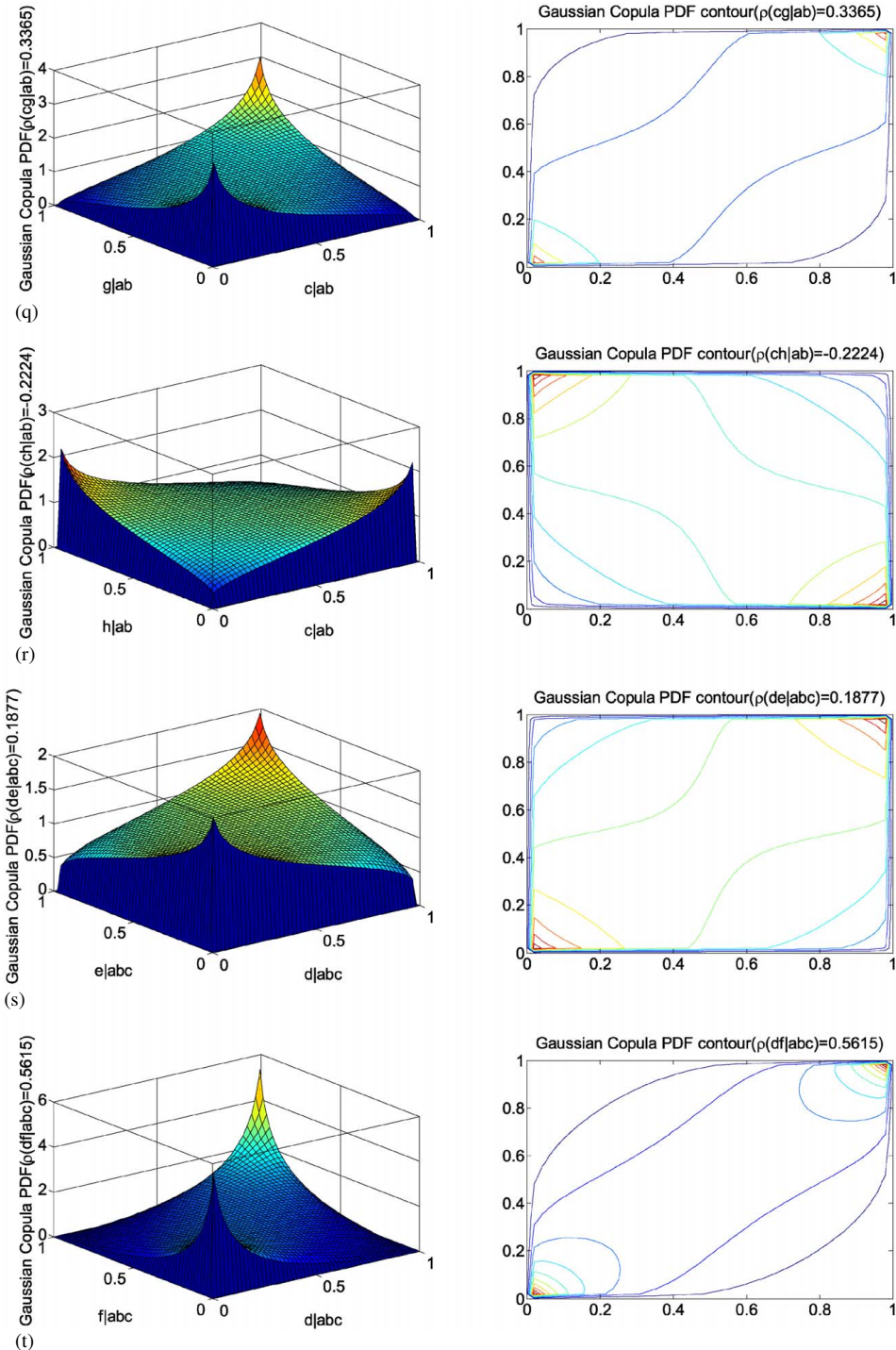


Fig. 8. (Continued.)

$$h_i(y_i) = [\sigma] - \gamma_P y_i, \quad i = 1, 2, \dots, n \quad (11)$$

be obtained with

$$\beta_i = \frac{\mu_{[\sigma]} - \gamma_P \mu_{y_i}}{\sqrt{\sigma_{[\sigma]}^2 + (\gamma_P \sigma_{y_i})^2}} \quad (12)$$

$$p_{fi} = \Phi(-\beta_i) \quad (13)$$

where h_i = the i th performance function; $[\sigma]$ = the strength (allowable stress); y_i = everyday extreme stress at the i th monitored point; and $\gamma_P = 1.15$ = the correction factor of the sensors. The everyday extreme stress mentioned in this paper refers to the maximum value of everyday monitored positive stresses and the absolute value of everyday monitored negative stresses.

In addition, with Eq. (10), reliability index (β_i) and the corresponding failure probability (p_{fi}) of the i th monitored point can

where $\mu_{[\sigma]}$ and $\sigma_{[\sigma]}^2$ = mean value and variance of $[\sigma]$, respectively; and μ_{y_i} and σ_{y_i} = mean value and standard variance of y_i , respectively.

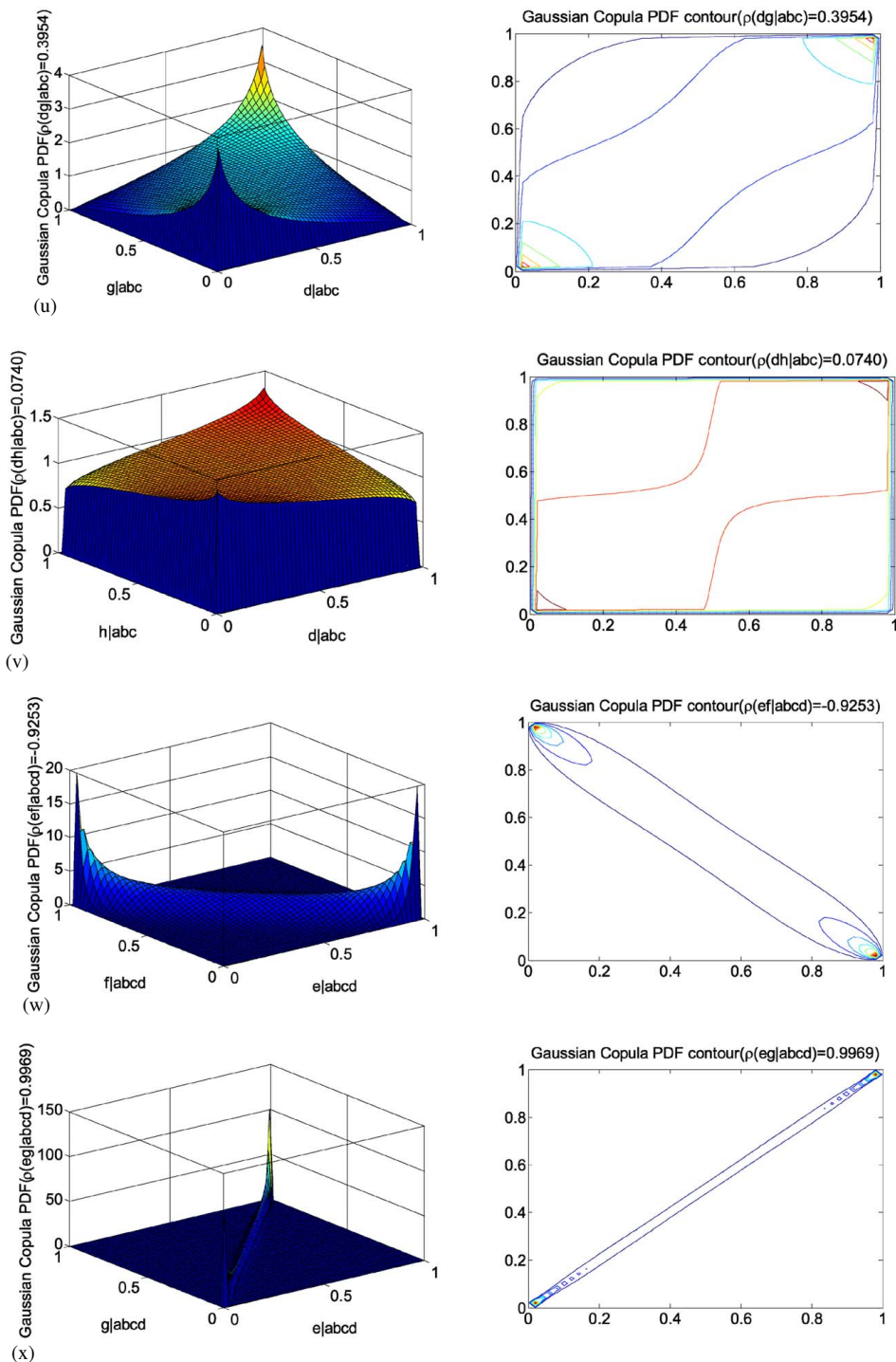


Fig. 8. (Continued.)

Failure Probability Analysis of Bridge Girder Section that Considers the Nonlinear Correlation of Failure Modes About Multiple Monitored Points

In this section, the pair-copula that considers the nonlinear correlation between the performance functions of any two monitored points is used to construct the vine copula model. This paper assumed that any system that was composed of two points was parallel. With Eq. (11), the failure probability of the parallel system that was composed of two monitored points can be solved with

$$\begin{aligned}
 P(h_i(X_i) \leq 0, h_j(X_j) \leq 0) &= P(H_i(h_i(X_i)) \leq H_i(0), H_j(h_j(X_j)) \leq H_j(0)) \\
 &= P(U_i \leq H_i(0), U_{j,t+1} \leq H_j(0)) \\
 &= C(H_i(0), H_j(0); \rho_{ij}) = C(p_{fi}, p_{fj}; \rho_{ij})
 \end{aligned} \tag{14}$$

where $H_i = \Phi\left(\frac{[\sigma] - y_i - \mu_i}{\sigma_i}\right)$, $H_j = \Phi\left(\frac{[\sigma] - y_j - \mu_j}{\sigma_j}\right)$, $H_i(0) = \Phi\left(\frac{-\mu_i}{\sigma_i}\right)$, $H_j(0) = \Phi\left(\frac{-\mu_j}{\sigma_j}\right)$, p_{fi} and p_{fj} can be computed with

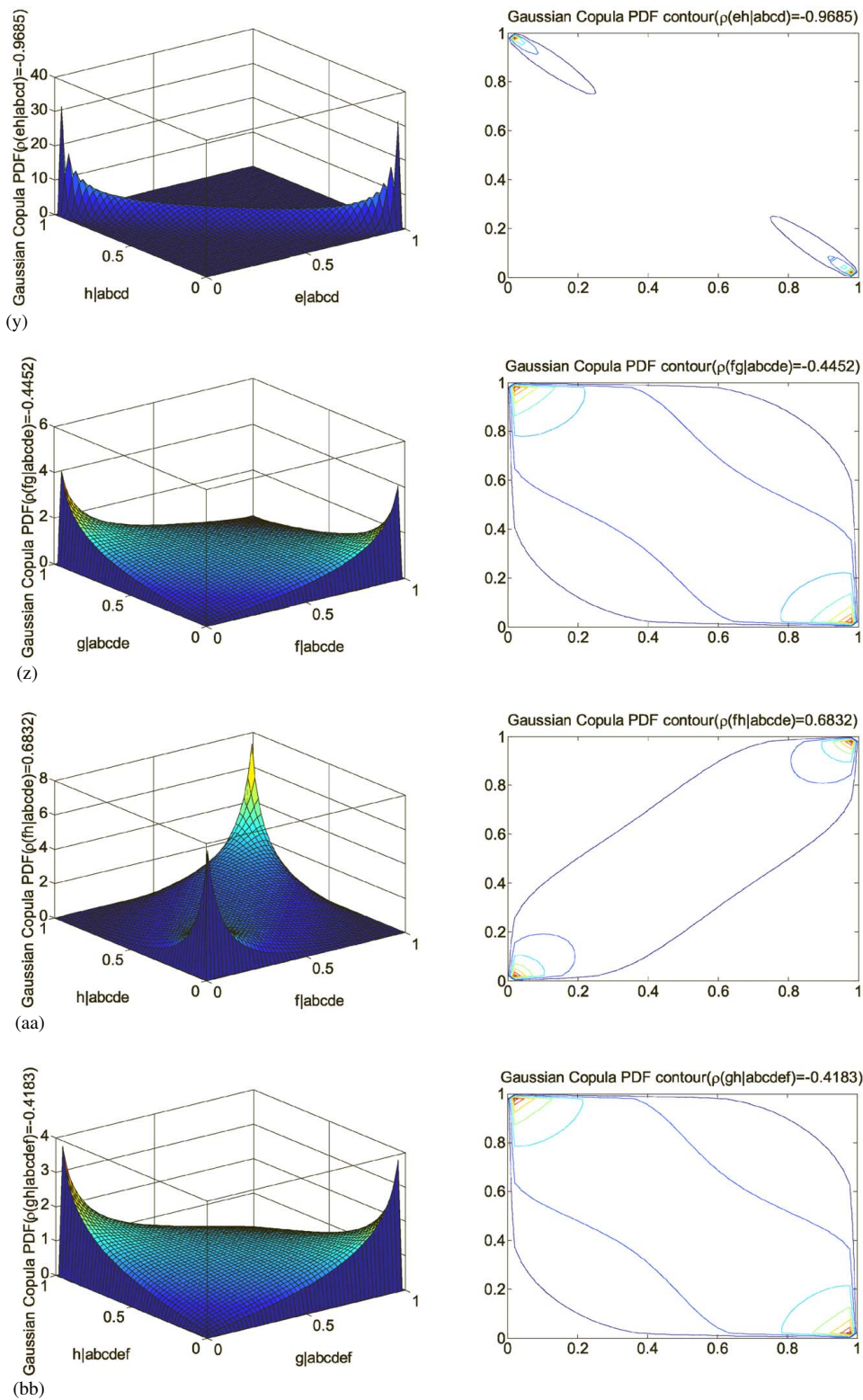


Fig. 8. (Continued.)

Eq. (13). C = copula function; and ρ_{ij} = the relevant parameter that can be obtained with Eq. (7). In this paper, C is the Gaussian copula function.

This paper supposed that the parallel systems, which were all composed of two monitored points, were serial. Therefore, with Eqs. (11)–(14), the failure probability of a bridge girder section that considered the nonlinear correlation of failure modes about

multiple monitored points can be solved with

$$P_{f_{\text{system}}} = \max_{i \neq j} \{C(p_{f_i}, p_{f_j}; \rho_{ij}), i, j = 1, 2, \dots, n, \text{ and } i \neq j\} \quad (15)$$

Therefore, the failure probability of a bridge girder section that does not consider the nonlinear correlation between multiple failure

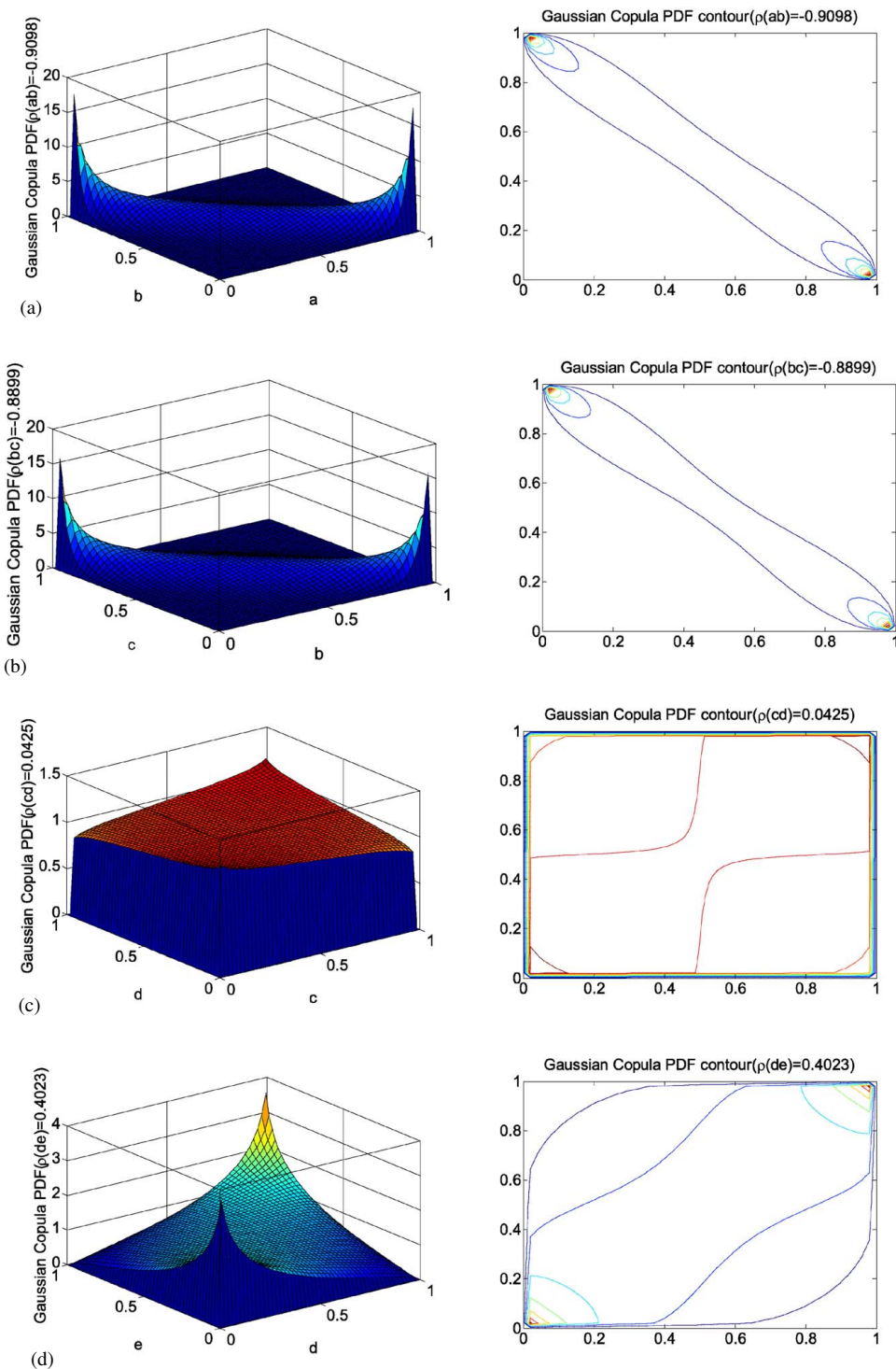


Fig. 9. PDF and contour plots of Gaussian copula functions for D-vine structure: (a) PDF and contour plots of Gaussian copula functions for C_{ab} ; (b) PDF and contour plots of Gaussian copula functions for C_{bc} ; (c) PDF and contour plots of Gaussian copula functions for C_{cd} ; (d) PDF and contour plots of Gaussian copula functions for C_{de} ; (e) PDF and contour plots of Gaussian copula functions for C_{ef} ; (f) PDF and contour plots of Gaussian copula functions for C_{fg} ; (g) PDF and contour plots of Gaussian copula functions for C_{gh} ; (h) PDF and contour plots of Gaussian copula functions for $C_{ac|b}$; (i) PDF and contour plots of Gaussian copula functions for $C_{bd|c}$; (j) PDF and contour plots of Gaussian copula functions for $C_{ce|d}$; (k) PDF and contour plots of Gaussian copula functions for $C_{eg|f}$; (l) PDF and contour plots of Gaussian copula functions for $C_{fh|g}$; (m) PDF and contour plots of Gaussian copula functions for C_{adbc} ; (n) PDF and contour plots of Gaussian copula functions for C_{belcd} ; (o) PDF and contour plots of Gaussian copula functions for C_{cdef} ; (p) PDF and contour plots of Gaussian copula functions for $C_{dg|ef}$; (q) PDF and contour plots of Gaussian copula functions for $C_{eh|fg}$; (s) PDF and contour plots of Gaussian copula functions for C_{aebcd} ; (t) PDF and contour plots of Gaussian copula functions for C_{bfcde} ; (u) PDF and contour plots of Gaussian copula functions for $C_{cg|def}$; (v) PDF and contour plots of Gaussian copula functions for $C_{dh|efg}$; (w) PDF and contour plots of Gaussian copula functions for C_{afbcde} ; (x) PDF and contour plots of Gaussian copula functions for $C_{bg|cdef}$; (y) PDF and contour plots of Gaussian copula functions for $C_{ch|defg}$; (z) PDF and contour plots of Gaussian copula functions for $C_{ag|bcdef}$; (aa) PDF and contour plots of Gaussian copula functions for $C_{bh|cdefg}$; and (bb) PDF and contour plots of Gaussian copula functions for $C_{ah|bcdefg}$.

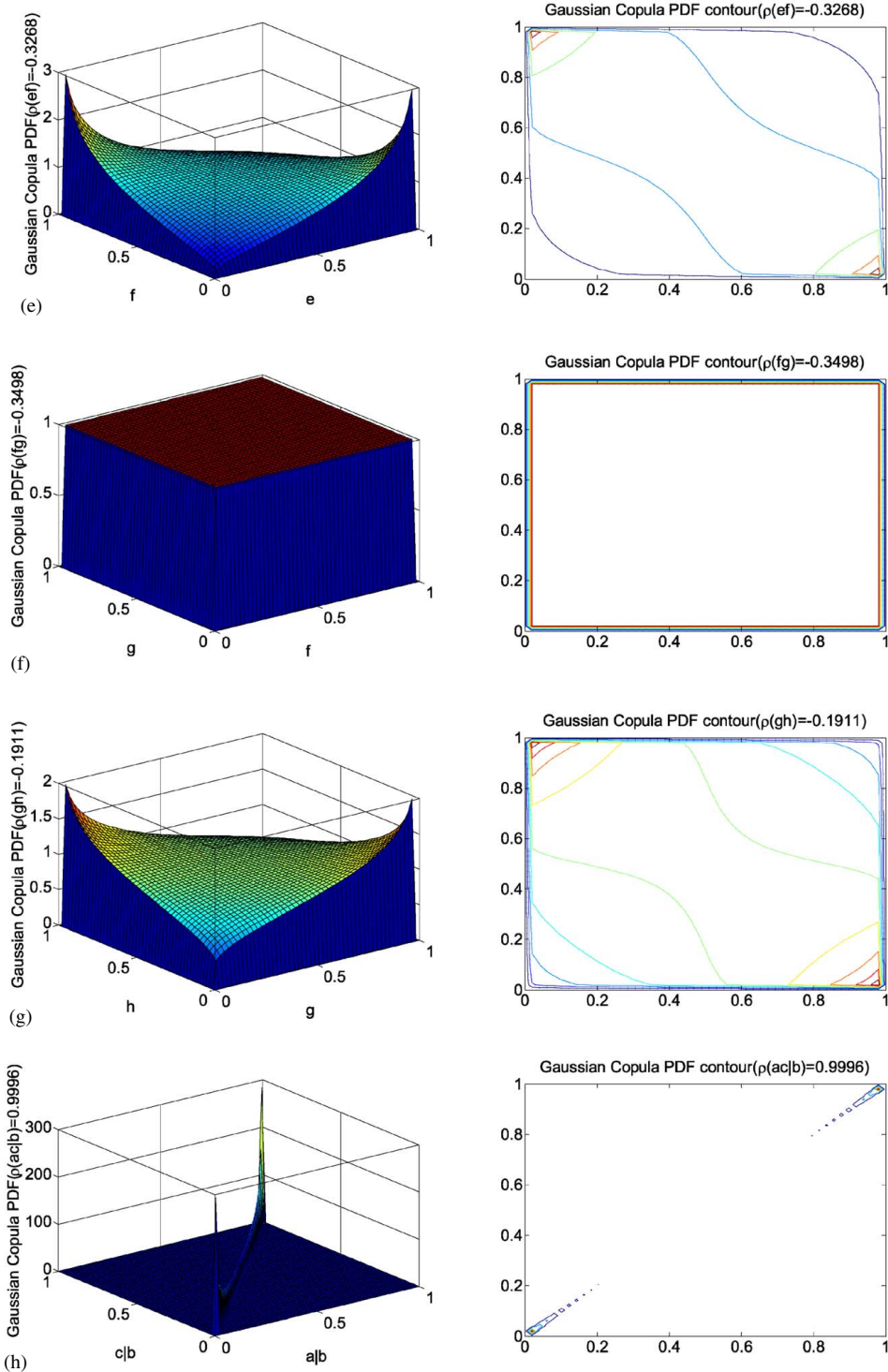


Fig. 9. (Continued.)

modes at multiple monitored points is

$$P_{f_{\text{system}}} = \max(p_{f_i}, i = 1, 2, \dots, n) \quad (16)$$

where $\max(\cdot)$ = the maximum value.

Application to an Existing Bridge

The Fumin bridge (Sun et al. 2016) in Tianjin, China is an unsymmetrical single-tower, self-anchored suspension bridge with

three-dimensional curved cables (Fig. 3). The deck mainly consists of a steel box girder with a short prestressed concrete segment at the right end anchorage; the main cables in the main span are anchored to the deck, and those in the side span on a vertical plane are anchored to the ground. Most parts of the bridge are made of steel.

The steel box girder system consists of an upstream girder, downstream girder and crossbeam. For the girder system, seven sections that include sections A–F were monitored, where, sections A, B, and G are in the side span; sections C, D, E, and F are in the main

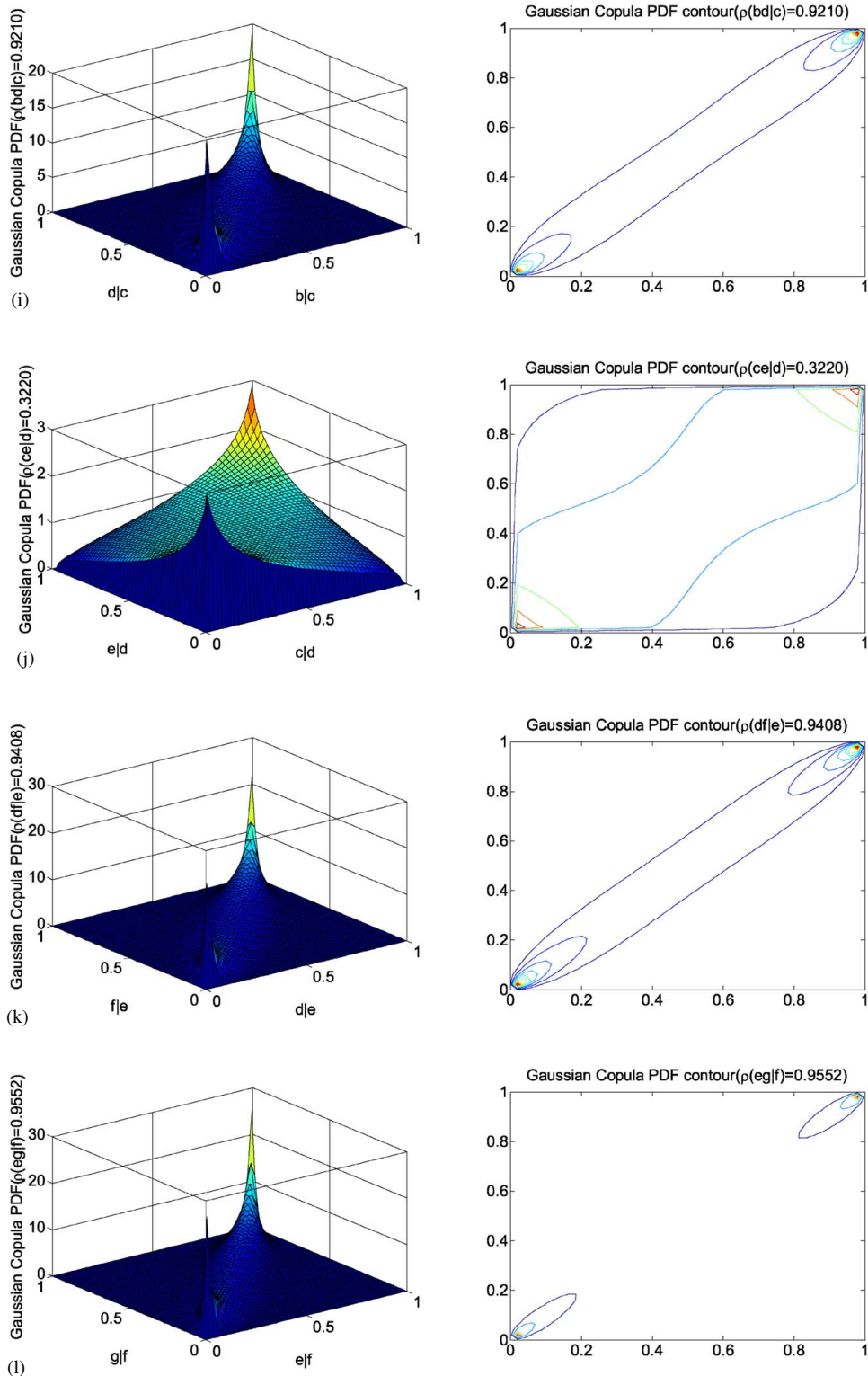


Fig. 9. (Continued.)

span. These sections are shown in Fig. 4. In the measurement programs for the girder system, the everyday extreme stresses about these seven sections are monitored through an array of stress sensors.

In this paper, the failure probability of section B (Figs. 4 and 5) was analyzed using the proposed vine copula model based on the monitored extreme stress data, the failure probability about sections B–G were solved with the same failure probability analysis method

with section B. The location of section B and the arrangement of the section sensors are respectively shown in Figs. 4 and 5. It can be seen from Fig. 5, that eight sensors were used to monitor the extreme stress of section B: FBG01049 and FBG01051 are at the inner side and the outer side of the upstream steel box girder top slab, respectively; FBG01050 and FBG01052 are at the inner side and the outer side of the downstream steel box girder

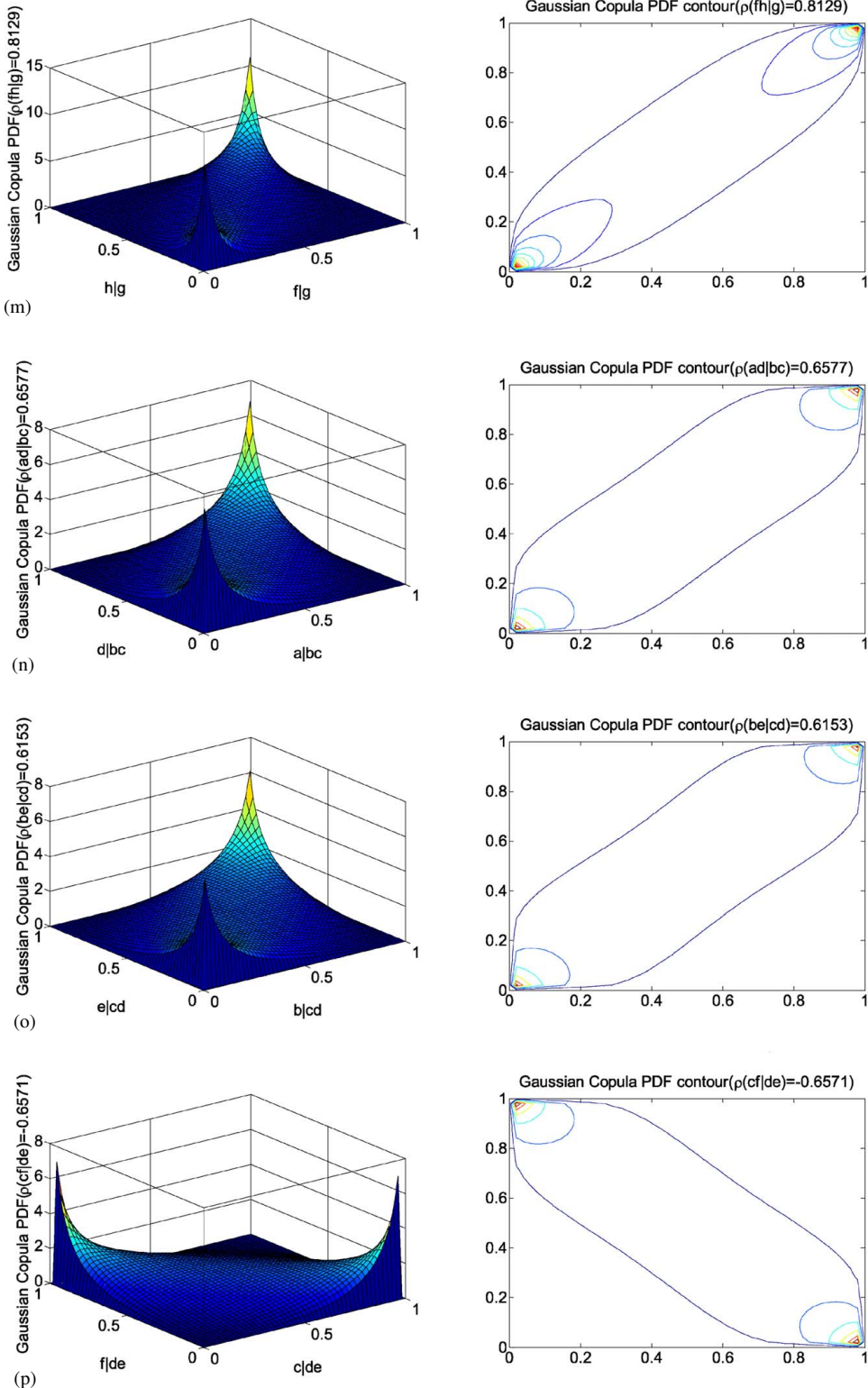


Fig. 9. (Continued.)

top slab, respectively; FBG01045 and FBG01048 are at the inner side and the outer side of the downstream steel box girder bottom slab, respectively; and FBG01047 and FBG01046 are at the inner side and the outer side of the upstream steel box girder bottom slab, respectively.

This paper used the extreme stress monitoring data for the eight monitoring points to analyze the failure probability of section B.

The everyday extreme stress information collected in this paper includes the stress information that was caused by vehicle load, temperature load, shrinkage creep and structural change, and the stress caused by structural weight was not included.

In this example, everyday extreme stresses at the four points were monitored for 1,000 days. The monitored points of FBG01047, FBG01049, FBG01046, FBG01051, FBG01045,

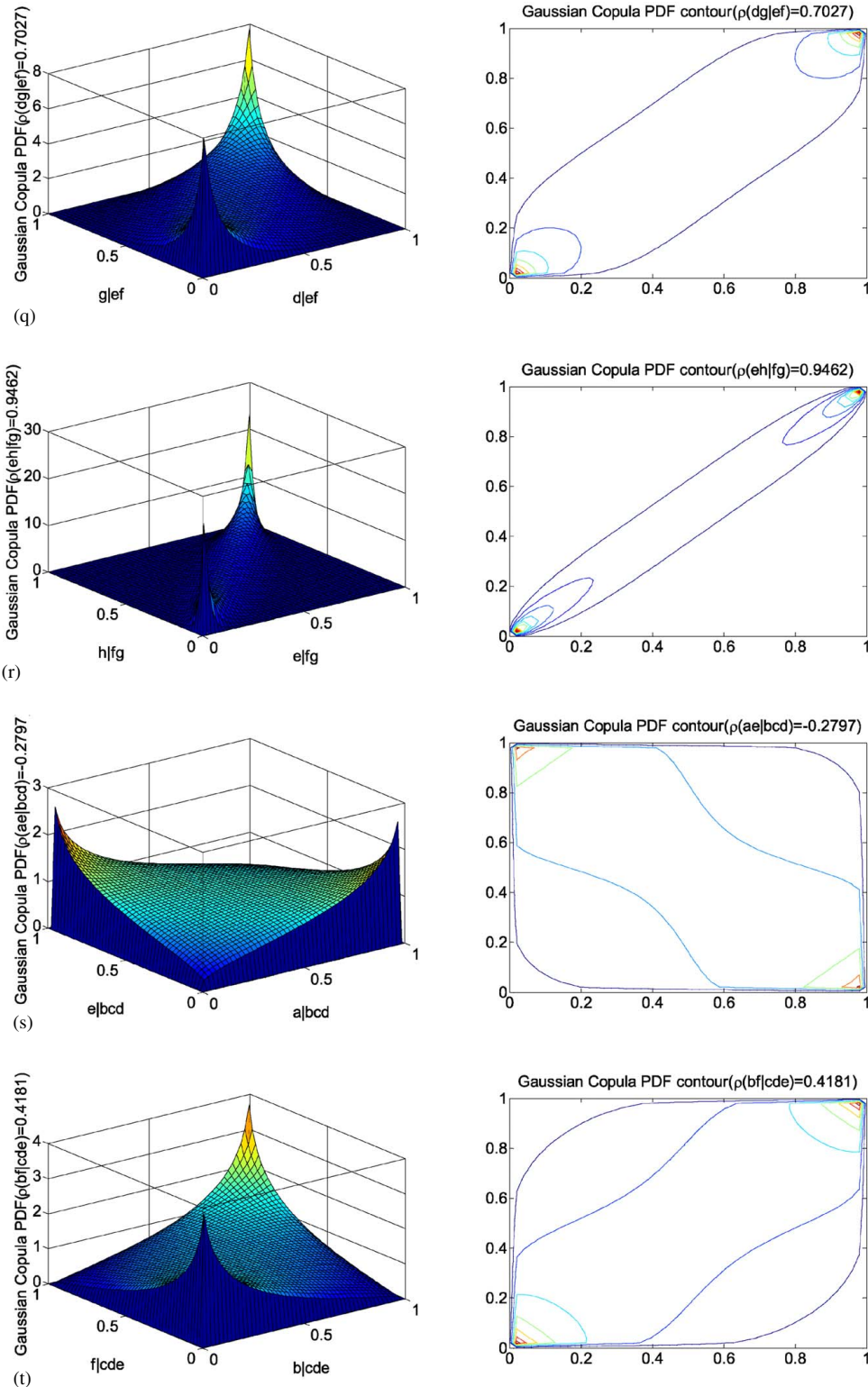


Fig. 9. (Continued.)

FBG01050, FBG01048 and FBG01052 correspond to a, b, c, d, e, f, g, and h, respectively and the monitored data is shown in Fig. 6. With this data, the PDFs, and CDFs about the four monitored variables that correspond to four monitored points were obtained.

For a bridge girder section, the allowable stress of steel follows a normal distribution with a mean value (411 MPa) and coefficient of

variation (0.098). Through the Kolmogorov–Smirnov (K–S) test, the monitored everyday extreme stress data about the four monitored points all approximately followed normal distributions that are shown in Fig. 7 and according to Frangopol et al. (2008a). The failure probability at each monitored point was computed with Eq. (13). The failure probability values of eight monitored points are respectively

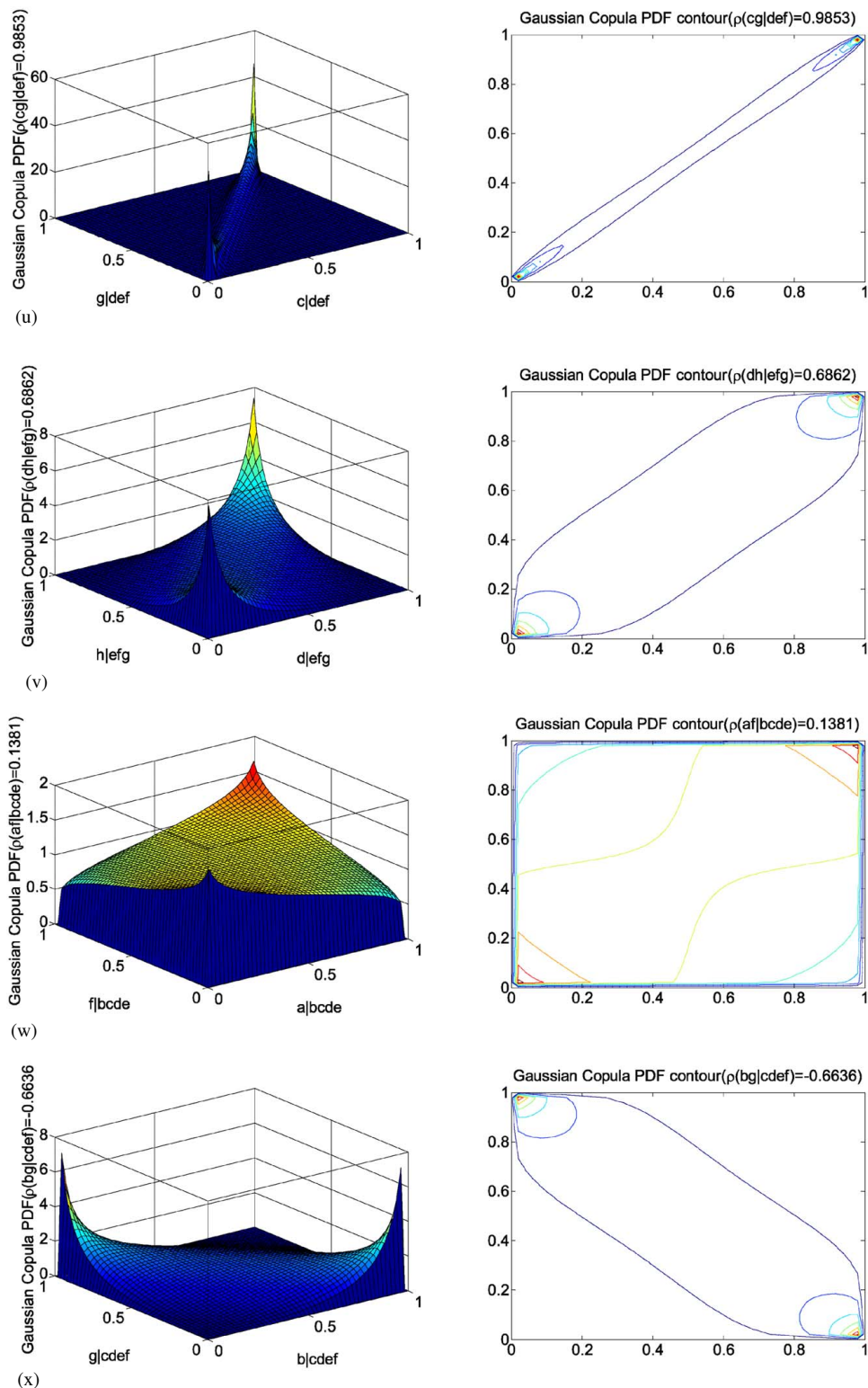


Fig. 9. (Continued.)

$$\begin{aligned}
 p_{fa} &= 1.44 \times 10^{-13}, p_{fb} = 2.68 \times 10^{-21}, \\
 p_{fc} &= 8.13 \times 10^{-22}, p_{fd} = 9.84 \times 10^{-23}, \\
 p_{fe} &= 3.02 \times 10^{-22}, p_{ff} = 2.31 \times 10^{-18}, \\
 p_{fg} &= 3.61 \times 10^{-21}, p_{fh} = 1.73 \times 10^{-21}
 \end{aligned}$$

The relevant parameters of the pair-copula can be obtained with Eq. (7) based on the monitored extreme stress data.

Based on this data, the following two cases were considered to analyze the reliability of section B. Case one did not consider the nonlinear correlation of failure modes about eight monitored points, the failure probability analysis of section B were solved with the maximum failure probability of the

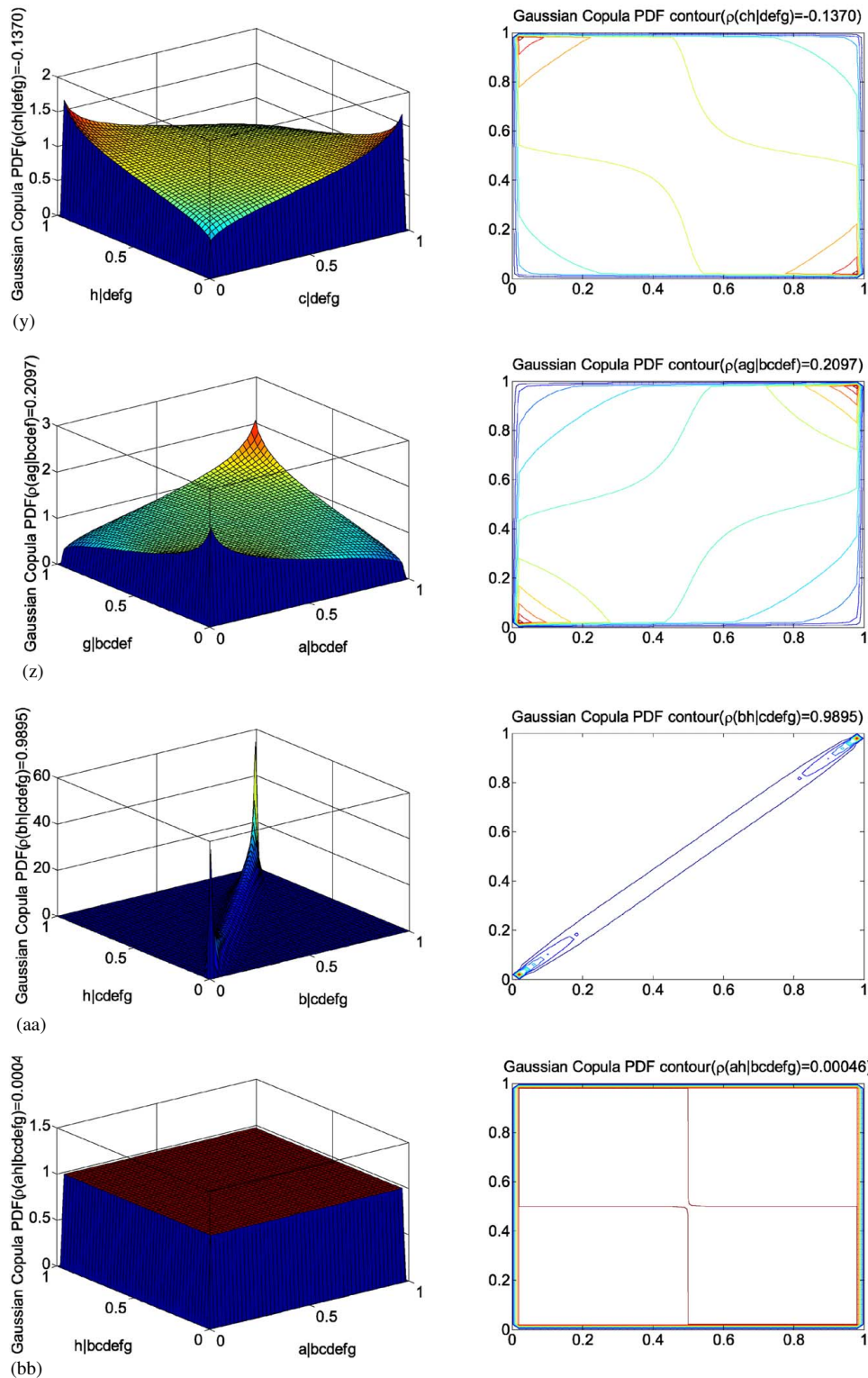


Fig. 9. (Continued.)

eight monitored points using Eq. (16), the maximum failure probability value was $p_{f_a} = 1.44 \times 10^{-13}$. Case two did consider the nonlinear correlation of failure modes about eight monitored points, the reliability analysis of section B were Eq. (15) based on Figs. 1 and 2.

For case two, C-vine and D-vine were applied to make the failure probability analysis of section B, respectively. C-vine based

system failure probability of section B was analyzed with the 28 pair-copula models shown in the edges of Fig. 1. The Gaussian copula PDFs and the corresponding contour plots are shown in Fig. 8, respectively that shows that nonlinear correlation exists between the failure modes of any two monitored points. Using Eq. (14), the failure probability of 28 pair-copula models can be obtained with

$$\begin{aligned}
p_{fab} &= 1.66 \times 10^{-43}, p_{fac} = 8.13 \times 10^{-22}, p_{fad} = 3.34 \times 10^{-35}, p_{fae} = 4.49 \times 10^{-39}, p_{faf} = 6.08 \times 10^{-36}, p_{fag} = 3.04 \times 10^{-26}, \\
p_{fah} &= 1.32 \times 10^{-38}, p_{fbc|a} = 1.54 \times 10^{-23}, p_{fbd|a} = 3.74 \times 10^{-23}, p_{fbe|a} = 8.52 \times 10^{-25}, p_{fbf|a} = 1.33 \times 10^{-26}, p_{fbg|a} = 1.56 \times 10^{-24}, \\
p_{fbb|a} &= 4.50 \times 10^{-22}, p_{fcclab} = 1.93 \times 10^{-49}, p_{fce|ab} = 3.39 \times 10^{-31}, p_{fcf|ab} = 1.77 \times 10^{-44}, p_{fcg|ab} = 3.16 \times 10^{-32}, p_{fch|ab} = 4.59 \times 10^{-45}, \\
p_{fde|abc} &= 1.16 \times 10^{-37}, p_{fdf|abc} = 7.77 \times 10^{-27}, p_{fdg|abc} = 1.26 \times 10^{-31}, p_{fdh|abc} = 1.11 \times 10^{-40}, p_{fef|abcd} = 2.97 \times 10^{-31}, p_{feg|abcd} = 3.02 \times 10^{-22}, \\
p_{fgh|abcd} &= 3.7 \times 10^{-35}, p_{fgl|abcde} = 3.12 \times 10^{-45}, p_{fhl|abcde} = 3.13 \times 10^{-24}, p_{fgh|abcdef} = 4.47 \times 10^{-48}
\end{aligned}$$

In addition, using Eq. (15), the failure probability for C-vine is $p_{fac} = 8.13 \times 10^{-22}$.

The D-vine based system failure probability of section B was analyzed with the 28 pair-copula models shown in the edges of Fig. 2. The Gaussian copula PDFs and the corresponding contour plots are shown in Fig. 9, which shows that a nonlinear correlation exists between the failure modes of any two monitored points. Using Eq. (14), the failure probability of 28 pair-copula models can be obtained with

$$\begin{aligned}
p_{fab} &= 1.66 \times 10^{-43}, p_{fbc} = 3.38 \times 10^{-50}, p_{fcd} = 3.83 \times 10^{-42}, p_{fde} = 3.06 \times 10^{-32}, p_{fef} = 1.24 \times 10^{-48}, p_{fkg} = 2.92 \times 10^{-47} \\
p_{fgh} &= 6.07 \times 10^{-45}, p_{fac|b} = 8.13 \times 10^{-22}, p_{fbd|c} = 1.97 \times 10^{-23}, p_{fce|d} = 2.26 \times 10^{-33}, p_{fdf|e} = 9.41 \times 10^{-23}, p_{feg|f} = 1.21 \times 10^{-22}, \\
p_{fjh|g} &= 1.10 \times 10^{-22}, p_{fad|bc} = 1.35 \times 10^{-23}, p_{fbe|cd} = 2.42 \times 10^{-27}, p_{fcf|de} = 3.78 \times 10^{-43}, p_{fdg|ef} = 2.99 \times 10^{-26}, p_{feg|fg} = 7.14 \times 10^{-23} \\
p_{fae|bcd} &= 1.19 \times 10^{-37}, p_{fbf|cde} = 3.42 \times 10^{-28}, p_{fcg|def} = 5.86 \times 10^{-22}, p_{fdh|efg} = 1.14 \times 10^{-26}, p_{faf|bcde} = 9.19 \times 10^{-28} \\
p_{fbg|cdef} &= 4.62 \times 10^{-45}, p_{fch|defg} = 1.02 \times 10^{-46}, p_{fag|bcdef} = 1.0 \times 10^{-28}, p_{fjh|cdefg} = 1.03 \times 10^{-21}, p_{fah|bcdefg} = 2.42 \times 10^{-34}
\end{aligned}$$

In addition, using Eq. (15), the failure probability for D-vine is $p_{fjh|cdefg} = 1.03 \times 10^{-21}$.

From the previous results: (1) the failure probability of section B that considered the nonlinear correlation of failure modes at monitored points was smaller than the one that did not consider nonlinear correlation, which proved that it was more reasonable and necessary to consider the nonlinear correlation of failure modes for failure probability analysis of bridge sections; (2) C-vine structure-based failure probability of bridge girder section was smaller than D-vine structure-based failure probability, because the C-vine structure assumed that the primary and secondary relationship existed for the failure modes of the multiple monitoring points, and the D-vine structure assumed that the relationship between the failure modes of the multiple monitoring points was equal. For the actual bridge girder section, the primary and secondary relationship usually exists for the failure modes of the multiple monitoring points; therefore, the C-vine structure-based failure probability analysis method was more reasonable.

Based on the previous failure probability analysis results, the C-vine structure-based failure probability analysis method was the most reasonable and section B is very safe.

Conclusions

In this paper, a new failure analysis method for bridge sections was proposed based on the Gaussian vine copula model and BHM extreme stress data, this method considered the nonlinear correlation of multiple failure modes at different monitored points. Through the illustration of monitored data for the existing bridge girder section, it was proved that: (1) failure probability of a bridge section that considered the nonlinear correlation of failure modes at different monitored points was smaller than when the nonlinear correlation of failure modes was not considered; (2) C-vine structure-based failure probability of a bridge girder section was smaller than the D-vine structure-based failure probability. For the actual bridge girder sections, the primary and

secondary relationship and nonlinear correlation usually exist for the failure modes of the multiple monitoring points; therefore, the C-vine structure-based failure probability analysis method was the most reasonable for failure probability assessment of bridge sections.

Data Availability Statement

All data generated or analyzed during this paper is included in this article.

Acknowledgments

The author would like to thank the editor and the anonymous reviewers for their constructive comments and valuable suggestions to improve the quality of the article. This work was supported by the National Key R & D Program of China (Grant No. 2019YFC1511005), Fundamental Research Funds for the Central Universities (Grant No. Izujbky-2020-55), and National Natural Science Foundation of China (Grant No. 51608243).

References

- Ang, A. H.-S., and W. H. Tang. 2007. Vol. 1 of *Probability concepts in engineering planning and design*. New York: John Wiley & Sons.
- Bedford, T., and R. M. Cooke. 2001. "Probability density decomposition for conditionally dependent random variables modeled by vines." *Ann. Math. Artif. Intell.* 32 (1–4): 245–268. <https://doi.org/10.1023/A:1016725902970>.
- Bedford, T., and R. M. Cooke. 2002. "Vines: A new graphical model for dependent random variables." *Ann. Stat.* 30 (4): 1031–1068. <https://doi.org/10.1214/aos/1031689016>.
- Catbas, F. N., M. Susoy, and D. M. Frangopol. 2008. "Structural health monitoring and reliability estimation: Long span truss bridge application with environmental monitoring data." *Eng. Struct.* 30 (9): 2347–2359. <https://doi.org/10.1016/j.engstruct.2008.01.013>.

- Dai, H. Z., and Z. G. Cao. 2017. "A wavelet support vector machine-based neural network metamodel for structural reliability assessment." *Comput.-Aided Civ. Infrastruct. Eng.* 32 (4): 344–357. <https://doi.org/10.1111/mice.12257>.
- Dissanayake, P. B. R., and P. A. K. Karunananda. 2008. "Reliability index for structural health monitoring of aging bridges." *Struct. Health Monit.* 7 (2): 175–183. <https://doi.org/10.1177/1475921708090555>.
- Fan, X. P. 2014. "Reliability updating and Bayesian prediction of bridges based on proof loads and monitoring data." Ph.D. thesis, School of Civil Engineering, Harbin Institute of Technology.
- Fan, X. P., and Y. F. Liu. 2018a. "A new dynamic prediction approach for the reliability indices of bridge members based on SHM data." *J. Bridge Eng.* 23 (12): 06018004. [https://doi.org/10.1061/\(ASCE\)BE.1943-5592.0001321](https://doi.org/10.1061/(ASCE)BE.1943-5592.0001321).
- Fan, X. P., and Y. F. Liu. 2018b. "Time-variant reliability prediction of bridge system based on BDGCM and SHM data." *Struct. Control Health Monit.* 25 (7): 1–16.
- Frangopol, D. M., A. Strauss, and S. Kim. 2008a. "Use of monitoring extreme data for the performance prediction of structures: General approach." *Eng. Struct.* 30 (12): 3644–3653. <https://doi.org/10.1016/j.engstruct.2008.06.010>.
- Frangopol, D. M., A. Strauss, and S. Y. Kim. 2008b. "Bridge reliability assessment based on monitoring." *J. Bridge Eng.* 13 (3): 258–270. [https://doi.org/10.1061/\(ASCE\)1084-0702\(2008\)13:3\(258\)](https://doi.org/10.1061/(ASCE)1084-0702(2008)13:3(258)).
- Liu, Y. F. 2015. "System reliability analysis of bridge structures considering correlation of failure modes and proof modes." Ph.D. thesis, School of Civil Engineering, Harbin Institute of Technology.
- Liu, Y. F., and X. P. Fan. 2016a. "Time-independent reliability analysis of bridge system based on mixed copula models." *Math. Probl. Eng.* 2016: 2720614. <https://doi.org/10.1155/2016/2720614>.
- Liu, Y. F., and X. P. Fan. 2016b. "Gaussian Copula-Bayesian dynamic linear model-based time-dependent reliability prediction of bridge structures considering nonlinear correlation between failure modes." *Adv. Mech. Eng.* 8 (11): 1–15.
- Liu, Y. F., X. P. Fan, and D. G. Lu. 2014. "Time-dependent uncertainty analysis of structures based on copula functions." In *Vulnerability, Uncertainty, and Risk: Quantification, Mitigation, and Management*, edited by M. Beer, S.-K. Au, and J. W. Hall, 1875–1887. Reston, VA: ASCE.
- Liu, Y. F., and D. G. Lu. 2014. "Reliability analysis of two-dimensional series portal-framed bridge system based on mixed copula functions." *Key Eng. Mater.* 574: 95–105. <https://doi.org/10.4028/www.scientific.net/KEM.574.95>.
- Melchers, R. E. 1987. *Structural reliability, analysis and prediction*. Chichester, UK: Ellis Horwood.
- Nelsen, R. B. 2006. An introduction to copulas. *Springer series in statistics*. Berlin: Springer.
- Ni, Y. Q., X. G. Hua, and J. M. Ko. 2006. "Reliability-based assessment of bridges using long-term monitoring data." *Key Eng. Mater.* 321–323: 217–222. <https://doi.org/10.4028/www.scientific.net/KEM.321-323.217>.
- Strauss, A., D. M. Frangopol, and S. Y. Kim. 2008. "Use of monitoring extreme data for the performance prediction of structures: Bayesian updating." *Eng. Struct.* 30 (12): 3654–3666. <https://doi.org/10.1016/j.engstruct.2008.06.009>.
- Strauss, A., A. M. Ivanković, J. C. Matos, and J. R. Casas. 2016. "Performance indicators for roadway bridges." In *Proc., 8th Int. Conf. on Bridge Maintenance, Safety and Management*, 965–970. Boca Raton, FL: CRC Press.
- Suda, J., A. Strauss, F. Rudolf-Miklau, and J. Hubl. 2009. "Safety assessment of barrier structures." *Struct. Infrastruct. Eng.* 5 (4): 311–324. <https://doi.org/10.1080/15732470701189498>.
- Sun, Y., H. P. Zhu, and D. Xu. 2016. "A specific rod model based efficient analysis and design of hanger installation for self-anchored suspension bridges with 3D curved cables." *Eng. Struct.* 110: 184–208. <https://doi.org/10.1016/j.engstruct.2015.11.040>.
- Wang, X. Y., and Y. Y. Lin. 2017. "Research on the correlation of bridge failure modes based on Copula function." *J. Transp. Sci. Eng.* 33 (2): 18–22.
- Zimmermann, T., A. Strauss, and K. Bergmeister. 2012. "Structural behavior of low-and normal-strength interface mortar of masonry." *Mater. Struct.* 45 (6): 829–839. <https://doi.org/10.1617/s11527-011-9801-2>.